Amyloidoma of the nasopharynx: CT and MR findings.

J L Hegarty and V M Rao

AJNR Am J Neuroradiol 1993, 14 (1) 215-218
http://www.ajnr.org/content/14/1/215

Amyloidoma of the Nasopharynx: CT and MR Findings

Joseph L. Hegarty[1] and Vijay M. Rao[1]

Summary: A case of nasopharyngeal amyloidoma with extensive skull base erosion is presented. CT revealed a large, relatively homogeneous, enhancing lesion; MR revealed a signal intensity iso- or slightly hyperintense compared to muscle on T1- and T2-weighted images, with a moderate degree of contrast enhancement. When an erosive mass is encountered at the skull base in a submucosal location in the nasopharynx, and MR demonstrates short T2 relaxation with signal iso- or slightly hyperintense relative to muscle, amyloidoma should be included in the differential diagnosis.

Index terms: Nasopharynx, computed tomography; Nasopharynx, magnetic resonance; Nasopharynx, neoplasms; Amyloidosis

Case Report

A 77-year-old man presented with a 1-month history of progressive left facial hypesthesia, diplopia, left facial paresis, left-sided deafness, dysphagia, hoarseness, left shoulder weakness, dysarthria, and difficulty with deglutition. He also complained of a long history of low back pain and a recent unexplained weight loss. Significant in his past medical history was a presumptive diagnosis of a cerebral vascular accident 9 months earlier, thought to explain his neurologic deficit. Physical examination confirmed involvement of cranial nerves V (V2 and V3) through XII on the left side, as well as spinal tenderness at the low thoracic level. Examination of the nasopharynx revealed a left-sided soft-tissue fullness with intact mucosa. A contrast-enhanced computed tomography (CT) scan of the head demonstrated a large, relatively homogeneous nasopharyngeal mass eroding the skull base, petrous apex, and internal auditory canal (Figs. 1A and 1B). The mass extended anteriorly into the left Meckel's cave and cavernous sinus as well as posteriorly into the left jugular foramen. T1- and T2-weighted axial MR images were obtained, confirming a large, submucosal mass extending from the left nasopharynx to the skull base, eroding through to the posterior fossa although not involving brain (Figs. 2A and 2B). The T1-weighted image revealed the mass to be isointense compared with surrounding muscle. The signal intensity of the mass decreased on the T2-weighted image, and was iso- or slightly hyperintense compared with muscle. MR images obtained after administration of gadopentate dimeglumine (0.1 mmol/kg) revealed moderate enhancement of the mass (Fig. 2C).

Further evaluation revealed an osteolytic soft-tissue mass at the T11 vertebral body with paraspinal and intraspinal extension on CT scan. A myelogram confirmed the spinal cord compression. Further evaluation of this osteolytic lesion with MR revealed imaging features similar to that of the skull base lesion. A bone marrow biopsy was performed to investigate the possibility of multiple myeloma and revealed numerous small, cleaved cells without plasma cells or amyloid stroma. The diagnosis of non-Hodgkin lymphoma was serendipitously made. Additional metastatic evaluation included: bone scan, CT brain, chest x-ray, CT chest, complete blood count with differential, sedimentation rate, full chemistry evaluation, prostatic acid phosphatase, and serum protein electrophoresis. All of these studies were within normal limits. Remarkably, there was no proteinuria and no lymphocyte subpopulation abnormalities. There was also no evidence of chronic inflammatory or infectious disease. Laboratory investigation weighed against a diagnosis of multiple myeloma. Although neither abdominal fat nor rectal biopsy were performed, systemic amyloidosis was ruled out by the absence of amyloid in the bone marrow specimen.

Biopsy of the nasopharyngeal lesion revealed a pink and white soft-tissue mass, histologically revealing an amyloid tumor with an associated atypical plasma cell infiltrate. Apple green birefringence of a Congo red-stained specimen con-

Received October 15, 1991; revision requested January 7, 1992; revision received and accepted March 23.

[1] Department of Radiology, Thomas Jefferson University Hospital and Jefferson Medical College, 1029 Main Building, 10th and Sansom Sts., Philadelphia, PA 19017, (215) 955-4804. Address reprint requests to Vijay M. Rao, MD.

AJNR 14:215–218, Jan/Feb 1993 0195-6108/93/1401-0215 © American Society of Neuroradiology

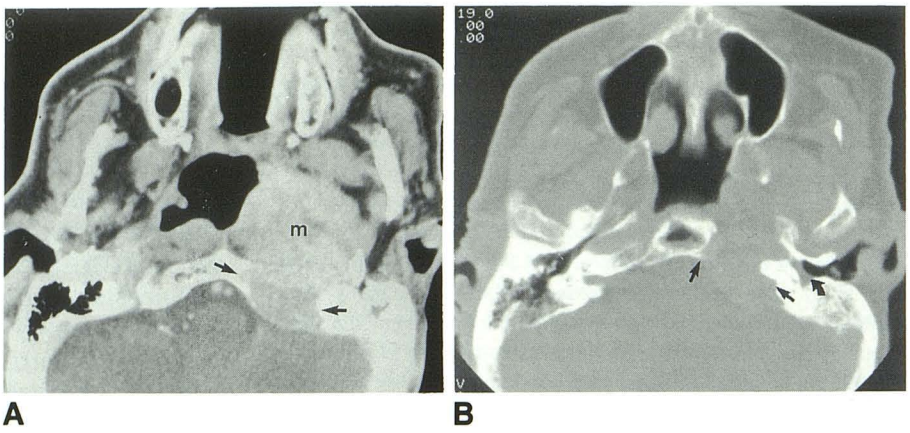

Fig. 1. *A*, Contrast-enhanced axial CT scan reveals a large, relatively homogeneous soft tissue mass (*m*) in the left nasopharynx. Note erosion of the skull base and similar density compared with surrounding musculature (*arrows*).

B, Axial CT scan at the level of the midnasopharynx. Bone windows confirm replacement of the left petrous apex and the internal auditory canal by amyloidoma (*arrows*). Soft-tissue density is seen in the middle ear cavity (*curved arrow*).

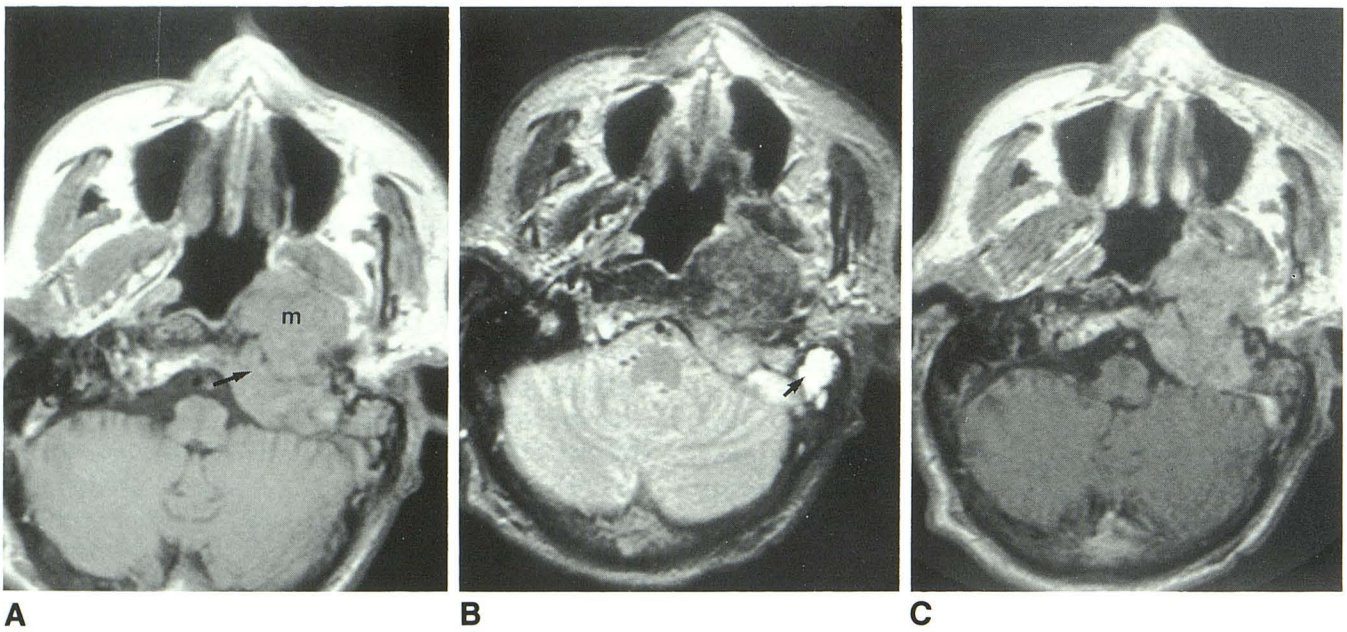

Fig. 2. *A*, T1-weighted (750/20/4) axial MR scan. The mass (*m*) shows a signal intensity equal to the adjacent musculature of the nasopharynx. Note the normal high signal intensity from the bone marrow is replaced by tumor at the skull base (*arrow*).

B, T2-weighted (2000/80/4) axial MR scan. The mass lies in a submucosal location, beneath a bright pharyngeal mucosa. The lesion demonstrates a signal intensity similar to or slightly higher than surrounding musculature. Note the markedly high signal intensity from the fluid in the left mastoid (*arrow*).

C, Contrast-enhanced T1-weighted MR image shows moderate enhancement throughout the mass.

firmed the presence of amyloid. Immunohistochemical analysis of the plasma cells revealed a polyclonal light chain (kappa and lambda) expression, weighing against a diagnosis of an extramedullary plasmacytoma.

The patient declined a biopsy of the thoracic spine and was offered palliative radiotherapy to his lower back lesion and systemic chemotherapy for his malignant lymphoma. The patient has had significant pain relief following radiotherapy to his back and continues systemic chemotherapy for malignant lymphoma. The nasopharyngeal amyloidoma remains unresected.

Discussion

The term "amyloidosis" describes the extracellular deposition of an organized, fibrillar matrix derived from normal serum protein polypeptides. Although the majority of amyloid deposits occur with preceding or concomitant systemic amyloidosis, localized amyloidosis continues to be discovered without systemic amyloidosis, especially in the head and neck.

The clinical classification of amyloidosis is often divided into systemic and localized forms (1, 2). Systemic amyloidosis comprises primary amyloidosis, secondary amyloidosis, and familial

amyloidosis. Primary amyloidosis includes amyloid deposition without preceding or coincident disease, with the exception of immunocyte dyscrasias such as multiple myeloma or Waldenstrom macroglobulinemia. Secondary amyloidosis includes amyloid deposition following or coincident with infectious, inflammatory, or neoplastic disease such as chronic osteomyelitis, rheumatoid arthritis, Hodgkin disease, and hypernephroma. Familial amyloidosis is a rare, hereditary form of systemic amyloidosis. Localized amyloidosis comprises both organ-limited amyloidosis and focal amyloidosis, both without associated systemic manifestations. Organ-limited amyloidosis is usually associated with increasing age, with deposits occurring in the lung, heart, brain, and skin. Focal amyloidosis (amyloidomas) are local amyloid deposits, often involving the head and neck. These local deposits are generally not associated with a plasma cell dyscrasia or systemic amyloidosis (3). The clinical significance of distinguishing systemic versus localized amyloidosis is that the localized forms do not limit life expectancy as systemic forms do (2).

Historically, localized amyloid deposits are most often described in the lung (1) although amyloid tumors have been identified in nearly every tissue in the body, including aerodigestive tract, bone, brain, breast, gasserian ganglia, gastrointestinal tract, extracranial head and neck, lymph nodes, orbit, pituitary gland, respiratory tract, skin, and urogenital tract (1, 3–5). In the head and neck, however, localized amyloid deposition is most common in the larynx (6). Amyloid localized to the nasopharynx is rare, reported in only seven previous cases in the literature (6–10).

The etiology of amyloidomas remains unclear. Many investigators believe these amyloid tumors arise from isolated, benign immunocyte clones of plasma cells, serving as the local producers of immunoglobulin light chains. Through subsequent enzymatic degradation, these polypeptides form amyloid fibrils in a connective tissue stroma (1, 2). Others believe these tumors arise from "burnt-out" extramedullary plasmacytomas (1). These hypotheses have been suggested since plasma cells and multinucleated giant cells are frequent histologic features of these local amyloid deposits. The diagnosis of amyloidoma is characteristically made when apple green birefringence is seen in polarized light following Congo red staining of the tissue (1, 6).

Although amyloidomas are considered benign tumors, they are aggressive, slow-growing lesions and when involving bone often produce osteolysis (11, 12). Amyloidomas involving bone are most often found at the thoracic vertebra (12), although they have also been reported involving the skull base three times previously in the literature (3–5). Ferrein et al, in 1990, reported a case of an erosive skull base amyloidoma involving the hypoglossal canal, clivus, and petrous temporal bone, resulting in multiple cranial nerve deficits (3). Matsumoto et al, in 1985, described a case of an amyloidoma in the cerebellopontine angle with erosion in the jugular foramen, also resulting in cranial nerve deficits (5). Giordano et al, in 1983, described an amyloidoma eroding the petrous temporal bone, clivus, occipital bone, foramen magnum, and cervical vertebra, with multiple cranial nerve deficits (4). Our case reveals similar bony erosion, involving petrous temporal bone, jugular foramen, and clivus. Cranial nerve deficits, however, were marked in our case, with involvement of cranial nerves V-XII. Interestingly, our case revealed synchronous diagnoses of non-Hodgkin lymphoma and localized amyloidosis. Although Hodgkin lymphoma is associated with the systemic form of amyloidosis, no association of amyloidosis has been documented with non-Hodgkin lymphoma, with the exception of one case report of a conjunctival amyloidosis with extranodal lymphoma (13).

Radiographic findings of amyloidomas are not well described. With bony involvement, conventional radiographs often reveal osteolysis. CT imaging of previously reported amyloidomas have shown patchy, hyperdense soft-tissue masses, occasionally with areas of localized calcification within the lesion (5, 11), and a slight degree of contrast enhancement (5, 14).

The MR signal characteristics of amyloidomas reflect the rather homogenous appearance of the amyloid matrix. The amyloidoma reveals a signal intensity equal to that of surrounding muscle on the T1-weighted image and remains iso- or slightly hyperintense compared with muscle on the T2-weighted image, unlike epithelial tumors. The orientation of the amyloid fibrils in a repeating beta-pleated fibrillar sheet configuration may account for this short T2 relaxation time, producing low signal on T2-weighted images. Following intravenous administration of gadopentate dimeglumine, the amyloidoma revealed a moderate degree of homogeneous enhancement.

Although nasopharyngeal amyloidomas are histologically benign lesions, they mimic aggressive tumors because of bone erosion at the skull

base. MR imaging provides a new glimpse at this radiographically elusive lesion. When a mass at the skull base demonstrates a short T2 relaxation similar to muscle in a submucosal location, an amyloidoma should be included in the differential diagnosis.

References

1. Glenner GG. Amyloid deposits and amyloidosis: the beta-fibrilloses. *N Engl J Med* 1980;302:1283–1292, 1333–1343
2. Kyle R, Greipp P. Amyloidosis: clinical and laboratory features in 229 cases. *Mayo Clin Proc* 1983;58:665–683
3. Ferrein JA, Bhuta S, Nieberg RK, Verity A. Amyloidoma of the skull base. *Arch Pathol Lab Med* 1990;114:974–976
4. Giordano A, Horne DG, Gudbrandsson F, Meyerhoff W. Temporal bone amyloidoma. *Otolaryngol Head Neck Surg* 1983;91:105–108
5. Matsumoto T, Tani E, Maeda Y, Natsume S. Amyloidomas in the cerebellopontine angle and jugular foramen. *J Neurosurg* 1985; 62:592–596.
6. Simpson GT, Skinner M, Strong MS, Cohen AS. Localized amyloidosis of the head and neck and upper aerodigestive and lower respiratory tracts. *Ann Otol Rhinol Laryngol* 1984;93:374–379
7. Kramer R, Som ML. Local tumor-like deposits of amyloid. *Arch Otolaryngol* 1935;21:324–334
8. Johner CH, Widen AH, Sahgal S. Amyloidosis of the head and neck. *Trans Am Acad Ophthalmol Otolaryngol* 1972;76:1354–1355
9. Kumagami H, Natzumura T, Aoki S. A case of nasopharyngeal amyloidosis. *Nippon Jibiinkoka Gakkai Kaiho* 1989;92:165–168
10. Kase Y, Linuma T, Shiono H, Iwasawa T. A case of nasopharyngeal amyloidosis. *Nippon Jibiinkoka Gakkai Kaiho* 1987;90:868–873
11. Pawar S, Kay C, Anderson H. Primary amyloidoma of the spine. *J Comput Assist Tomogr* 1982;6:1175–1177
12. Leeson MC, Rechtine GR, Makley JT, Carter JR. Primary amyloidoma of the spine: a case report and review of the literature. *J Comput Assist Tomogr* 1985;10:303–306
13. Marsh WM, et al. Localized conjunctival amyloidosis associated with extranodal lymphoma. *Opthalmology* 1987;94:61–64
14. Cohen AS, Lessel S. Amyloid tumor of the orbit. *Neuroradiology* 1979;14:157–159